Sensors and Materials, Vol. 12, No. 6 (2000) 375–388
MYU Tokyo

S & M 0416

Development of Si Monolithic Ferroelectric-Microbolometer Using Pulsed-Laser-Deposited (Ba, Sr)TiO_3 Thin-Film for Uncooled Chopperless Infrared Sensing

Minoru Noda*, Huaping Xu[1], Tomonori Mukaigawa[2], Hong Zhu, Kazuhiko Hashimoto[3], Hiroyuki Kishihara[4], Ryuichi Kubo[5], Tatsuro Usuki[6] and Masanori Okuyama

Dept. of Physical Science, Graduate School of Engineering Science, Osaka University, 1-3 Machikaneyama-cho, Toyonaka Osaka 560-8531, Japan
[1]Technology Research Institute of Osaka Prefecture, 2-7-1 Ayumino, Izumi, Osaka 594-1157, Japan
[2]Fundamental Res. Sect., R & D Labs., Hochiki Corp., 246 Tsuruma, Machida, Tokyo 194-0004, Japan
[3]Human Environment System Development Center, Matsushita Electric Industrial Co. Ltd., 3-1-1 Yagumo-nakamachi, Moriguchi, Osaka 570-8501, Japan
[4]Shimazu Corp., 3-9 Hikaridai, Seika-cho, Soraku-gun, Kyoto 619-0237, Japan
[5]R & D Division, Murata Mfg. Co. Ltd., 2288 Ohshinohara, Yasu, Shiga 520-2393, Japan
[6]New Materials Res. Center, Sanyo Electric Co. Ltd., Hirakata, Osaka 573-8534, Japan

(Received August 7, 2000; accepted October 4, 2000)

Key words: BST ferroelectric thin film, dielectric bolometer, ferroelectric microbolometer, thermal image sensing, uncooled infrared image sensor, micromachining, thermal isolation membranes, monolithic process, pulsed laser deposition, grain-size effect

$(Ba_{0.75}Sr_{0.25})TiO_3$ (BST) has been prepared at 520°C in thin-film form by pulsed laser deposition and shows a large temperature coefficient of dielectric constant (TCD) adequate for application in a dielectric bolometer imager. Pixels of capacitance-capacitance (C-C) balanced BST thin-film microbolometers have also been fabricated by integrating Si-bulk micromachining and ferroelectric thin-film processing. The film shows bolometric behavior with TCD values of 1%/K, which is much lower than that in bulk, but chopperless operation of pixels of microbolometers so fabricated was confirmed. Finally, the dielectric bolometer (DB)-mode operation in the detector pixel was confirmed for the

*Corresponding author, e-mail address: noda@ee.es.osaka-u.ac.jp

integrated device structure, and the resultant voltage sensitivity (R_v) and specific detectivity (D^*) were observed and calculated to be about 0.8 kV/W and 1.6×10^8 cmHz$^{1/2}$/W with a noise voltage (V_n) of 100 nV, respectively, when the detector size was 200 μm square and the top IR absorber was Au-black.

1. Introduction

Recently, development of highly sensitive, low-cost, uncooled thermal detectors and imagers based on integrated microbolometer array technology has increasingly become a mainstream activity in the field of infrared (IR) sensing.[1–6] The recent advances in silicon micromachining further drive microbolometer technology into an exciting area. The ultimate noise equivalent temperature difference (NETD) has been reported to be about 2 to 5 mK for a typical case set by an uncooled thermal detection mechanism, considering the background fluctuation noise limit.[3] To attain the ultimate NETD, various new monolithic schemes have been envisioned for integrating advanced sensor material processes and micromachining techniques with existing on-chip Si-readout technology. VO_x-based resistive bolometer arrays fabricated on surface micromachined Si readout IC substrates have recently enabled many companies to market their infrared cameras with NETD-values near 80 mK.[1,2] The advanced dielectric approach of hybrid ferroelectric microbolometer arrays[3,4] has challenged the NETD record down to 38 mK due to the superhigh thermal response of ferroelectric BST ceramics enhanced by electric bias. This technology will surely evolve along the mainstream of micromachining and on-chip integration in a fashion similar to that in approaches to resistive microbolometers.

Since monolithic ferroelectric microbolometer technology has the potential to achieve the lowest NETDs, a comprehensive suite of key technologies was intensively developed. The critical features are thermal confinement design (including thermal isolation and $\lambda/4$ resonant absorption mechanisms) and microfabrication of robust element-bridge arrays with a high fill-factor and small pitch size, thin-film processing of ferroelectric films with minimum degradation of bolometric performance, and optimization and monolithic implementation of readout schemes. Thus we have launched studies geared to prototyping a new type of ferroelectric microbolometer with an emphasis on demonstrating the feasibility of integrating MOSFET processes along with Si-bulk micromachining and ferroelectric thin-film processing into the fabrication.

This paper highlights: 1) the superiority of thermal detection by ferroelectrics operating in a dielectric bolometer (DB) mode;[4–6] 2) a new pixel structure consisting of a balanced pair consisting of a detecting capacitor and a reference capacitor, as well as a novel pulse-biased operation mode, which is explained and compared with the other DB modes; 3) a two-step micromachining technique (i.e., tetramethyl ammonium hydroxide (TMAH) pre-etching and final SF_6 Reactive Ion Etching) and stress-balanced SiO_2/SiN/SiO_2-stacked membrane structure; 4) sensor material of ferroelectric BST (Ba/Sr=75/25) films prepared by pulsed laser deposition (PLD) and employed in the fabrication of the pixel bolometers; 5) success in a process integration test that proved good compatibility

among MOSFET processes, Si-bulk micromachining and BST thin-film processing, and finally 6) infrared (IR) responses in DB mode operation that confirmed good detectivities.

2. Operating Mode in a Dielectric Bolometer-Type Detector Pixel

Pulsed mode operation offers the advantage of chopperless operation because it electrically releases the temperature-dependent pyroelectric charge on a ferroeletctric capacitor,[3] whereas both inherent (i.e., no bias applied) and electric-field-induced (DC-mode) pyroelectric operations need a chopper.

Conventionally, both the inherent and induced pyroelectric mode operations have used one ferroelectric capacitor in a pixel, and the resultant pyroelectric current becomes a direct output after IR absorption. Figure 1(a) shows our proposed IR detector pixel circuit.[5,6] Our detection circuit consists of a serially connected pair consisting of an IR detecting ferroelectric capacitor and a reference ferroelectric capacitor comprising a differential capacitance ratio circuit. We intend to detect a voltage change as a result of a change in dielectric constant of the ferroelectric film in the detector, so the film is also quite usable even at temperatures above the Curie temperature (T_c), where the ferroelectricity is lost in the film.

It is also possible, by DC-mode biasing of the two capacitors, for the proposed circuit in Fig. 1(a) to attain the voltage output change after IR absorption without a chopper. Note that the output voltage change in the DC-mode is basically the same as that in the pulsed mode. However, associated with the continuously applied electric field in the DC

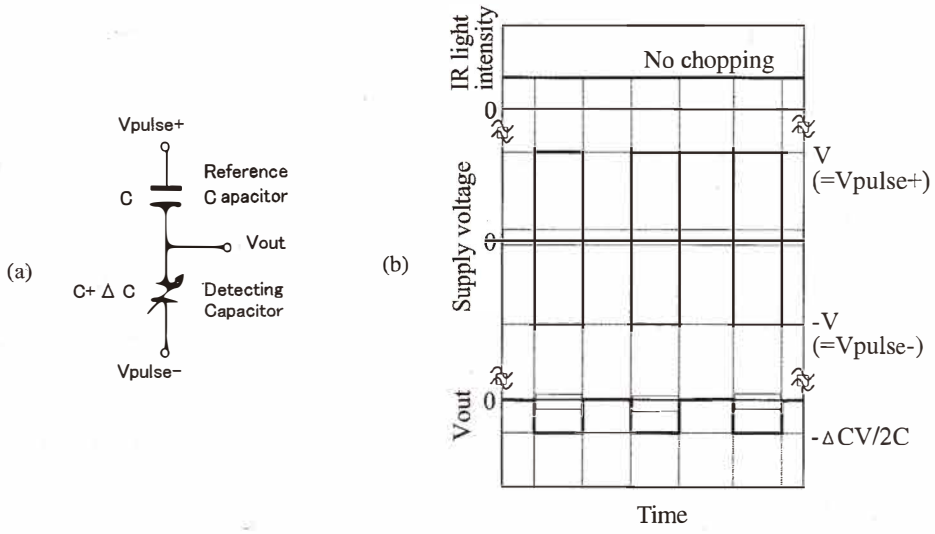

Fig. 1. (a) Serially connected capacitor-capacitor circuit used in our pulsed mode dielectric bolometer-type detector pixel and (b) timing charts of IR light intensity, supply voltage and output voltage in the circuit shown in (a).

mode, a continuous leakage current through the ferroelectric becomes a serious problem in detecting low-level signals especially for focal plane arrays. On the other hand, the electric field stress and the resultant leakage become much reduced in the pulsed mode especially as the time width ratio in the OFF state of the pulse period increases. Figure 1(b) shows timing charts of IR light intensity, supply voltage and output voltage in our pulsed mode dielectric bolometer detector pixel. The output voltage change is proportional to the capacitance change ΔC, which originates from changes in dielectric constant in the ferroelectric film after IR absorption.

3. Process Design and Fabrication

The technical approach to the development of our ferroelectric microbolometer is to extend both the high-temperature processing of ferroelectric thin-film and the sensor micromachining methods to allow the compatible integration of on-chip electronics. The process design as well as the resultant structure of our Si-monolithic BST thin-film microbolometer was developed, as shown in Fig. 2. Generally, the Si substrate is monolithically separated into two areas allocated for MOSFETs and membranes. The silicon underneath the sensitive part is anisotropically etched from the back surface of the wafer leaving a SiO_2/SiN/SiO_2 membrane supported over the etched groove. Accordingly, this groove should be aligned so that sensing capacitors are positioned in the center of the membrane and are thus thermally isolated from the silicon substrate. Another capacitor for the reference should be positioned on the thick Si wafer working as a heat sink.

3.1 *Process sequence of microfabrication*

The process sequence illustrated in Fig. 2 was implemented and established as a fabrication flow showing total compatibility. Two-faced mirrored Si-wafers with either a <110>- or <100>-orientation were used in the fabrication. When using the <100>-oriented Si-wafers, the aligned grooves are "V"-shaped in contrast to the "H"-shaped ones in <110>-oriented wafers. The major steps in the processing sequence are summarized as follows:

(1) The LOCOS process was used to define the areas for MOSFETs and membranes. The field oxide for membranes was patterned and etched back by a buffered hydrofluoric acid (BHF) to leave a thin layer of SiO_2 around 150 nm thick.

(2) MOSFETs were fabricated by standard IC processes. The SiN layer was used not only as a passivation layer for subsequent Si anisotropic etching in TMAH, but also served as a layer to balance the total stress in the resultant SiO_2/SiN/SiO_2 layer-stacked membrane because of its expansive stress on the Si wafer. The deposition of SiN is controlled to be about 250 nm thick.

(3) SiO_2(NSG) about 800 nm thick was formed by LPCVD, then the nondoped silica glass (NSG) was patterned and removed by BHF to form a stacked NSG(800 nm)/SiN (250 nm)/SiO_2 (150 nm) layer in the area for the membranes.

(4) Patterns of Si-windows on the back surface of the wafer were formed and anisotropic etching of Si in TMAH at 104°C was carried out. This etching was precisely controlled to

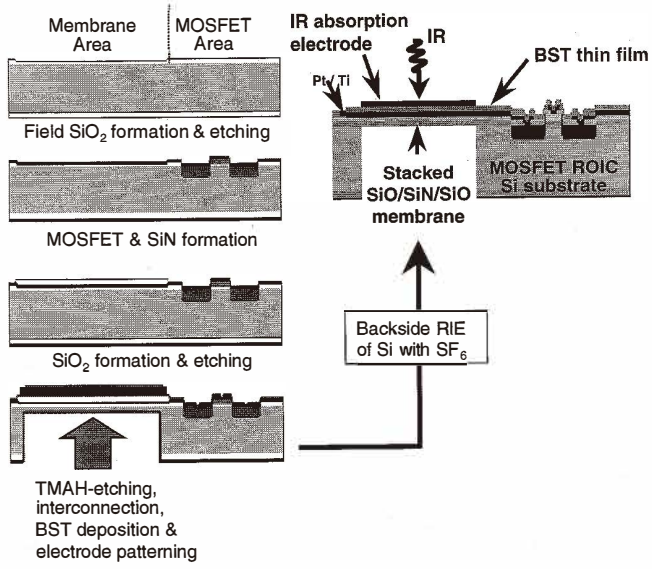

Fig. 2. Monolithic process sequence in the fabrication of micromachined ferroelectric bolometers.

form grooves or narrow trenches with Si 50-μm-thick remaining. This 50-μm-thick Si is essentially important to assure that the etched wafer is strong enough for manipulations in following processes.

(5) The interconnection of MOSFETs as well as the bottom electrode patterns for ferroelectric capacitors were formed with Pt/Ti. Then BST film was deposited by PLD and the upper electrode of Pt/Ti was patterned to form sensing and reference BST thin-film capacitors. After that, an additional dry-etching by RIE with SF_6 from the backside of the chips or wafers was performed to remove all the remaining 50 μm-thick Si. In this way, the sensing capacitors supported only by SiO_2/SiN/SiO_2 trilayer-stacked diaphragms were formed and BST thin-film bolometer sensors were monolithically realized.

A completed BST-bolometer array on a <110>-oriented Si-wafer is shown in Fig. 3(a), ready for wire bonding and IR-sensing characterizations on our standardized IR-test board. Figure 3(b) also shows a micrograph of a part of the fabricated 1×8 linear array on a monolithic test chip. The element size of sensing and reference capacitors was optimized to be 200×200 μm^2 based on our existing process conditions. Although BST film on the order of one micron thick is optimal for thin-film IR-sensors, the film acquired successfully thus far on our micromachined Si-wafers is limited to a thickness less than 0.4 μm. Film cracking tends to occur on the substrate surface when BST film is thicker than the critical value of about 0.4 μm.

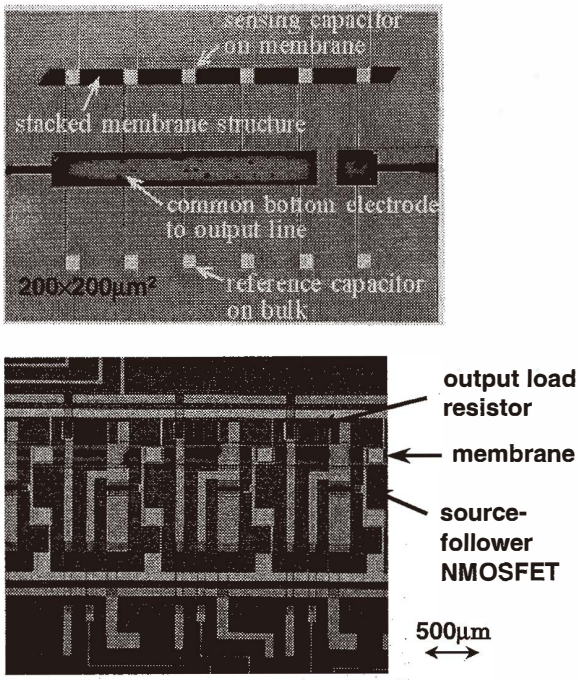

Fig. 3. Photographs of (a) an as-fabricated 1 × 5 linear test array and (b) an 1 × 8 linear test array monolithically integrated with a source-follower NMOSFET and an output load resistor.

3.2 *PLD-deposited BST films and its characterization*

PLD is recognized as a powerful tool which enables the preparation of ferroelectric oxide films with good stoichiometry. It has the feature of comparatively low-temperature deposition of well-crystallized films. Therefore, PLD is preferred for our work. In addition, PLD has been employed as a pilot process to test the compatibility of ferroelectric thin-film processing with monolithic processes. Details on PLD preparation of BST thin films were described elsewhere.[7]

As shown in Fig. 4, a microscopic view of the micromachined membrane from the surface and back of the substrate shows a flat and crack-free image, indicating the stress within the membrane is well balanced, where the sensing capacitor of Pt/Ti/BST/Pt/Ti is supported on the SiO_2/SiN/SiO_2 transparent membrane.

Figure 5(a) shows X-ray diffraction (XRD) patterns. Film crystallinity depends strongly on O_2 pressure at a laser fluence of 1.5 J/cm^2 and T_{sub}=550°C. Perovskite (100)-orientation prevails at 20 mTorr while the (110)-orientation tends to be preferred when the pressure increases. The chemical activity of oxygen radicals generated in low-pressure O_2 ambient is believed to be higher than in high pressure O_2 ambient. However, an undesired BaO_x phase appears when O_2 pressure reaches 0.1 Torr. Figure 5(b) shows the effect of laser fluence on film crystallinity. The BaO_x-phase could be removed simply by increas-

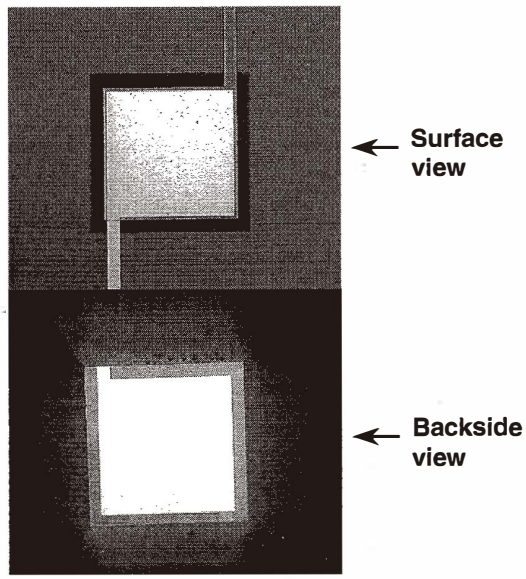

Fig. 4. Membrane parts observed from both surface and backside of the chip.

ing laser fluence. A plasma plume is generated by laser irradiation and increases with increasing fluence. This fact suggests that the plasma plume created at a higher fluence is better than that at lower fluences in stoichiometry transfer. Thus, high fluence and low O_2 pressure favor the formation of a good crystalline perovskite phase. A fluence of around 2 J/cm^2 is high enough for depositing pure perovskite BST thin films in an O_2 ambient lower than 0.1 Torr. Figure 5(c) shows the XRD patterns of BST films deposited at a fluence of 2 J/cm^2 and various T_{sub} and O_2 pressures. It is confirmed that T_{sub} higher than 520°C is adequate for perovskite formation, while lower O_2 pressure favors the (100)-orientation. An O_2 pressure of 20 mTorr is better than either 50 mTorr or 0.1 Torr.

The dependence of ferroelectricity on T_{sub} as well as grain size was investigated by measuring D-E hysteresis loops and ε_r (tand δ) -T curves and characterizing surface morphology by atomic force microscopy (AFM), because higher T_{sub} favors crystal growth and the ferroelectric properties of BST thin film strongly depend on its crystallinity. According to Figs. 6 and 7, higher T_{sub} produces higher ε_r and larger grains and increases TCD. All the films give slim hysteresis loops corresponding to the typical superparaelectric nature of very diffusive ferroelectric phase transitions with high ε_r. This behavior is similar to that of a relaxor-type ferroelectric material, whose BST films actually lost their profound ferroelectricity at room temperature because the maximum grain size as achieved by PLD at 550°C is about 100 nm, not yet exceeding the critical value of 0.2 μm in the bulk ceramic.[7] As a result, the T_c of the film is greatly shifted down from around 50°C in its bulk ceramic form. Thus far the maximum TCD value at 25°C in 550°C-deposited films is about –0.3%/K.

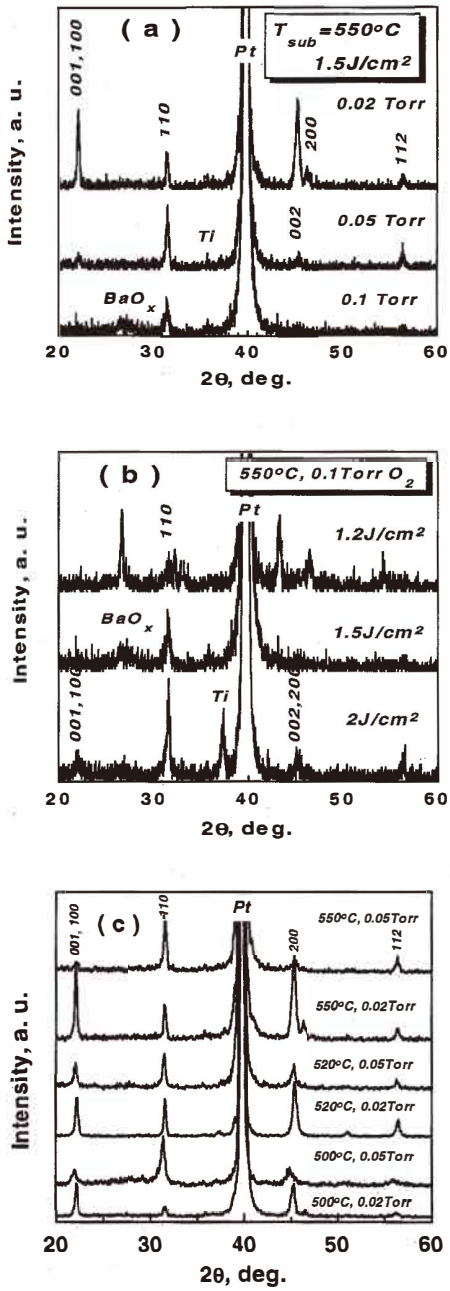

Fig. 5. XRD patterns of BST films deposited at different (a) O_2 pressures, (b) laser fluence and (c) T_{sub} to locate the optimal conditions.

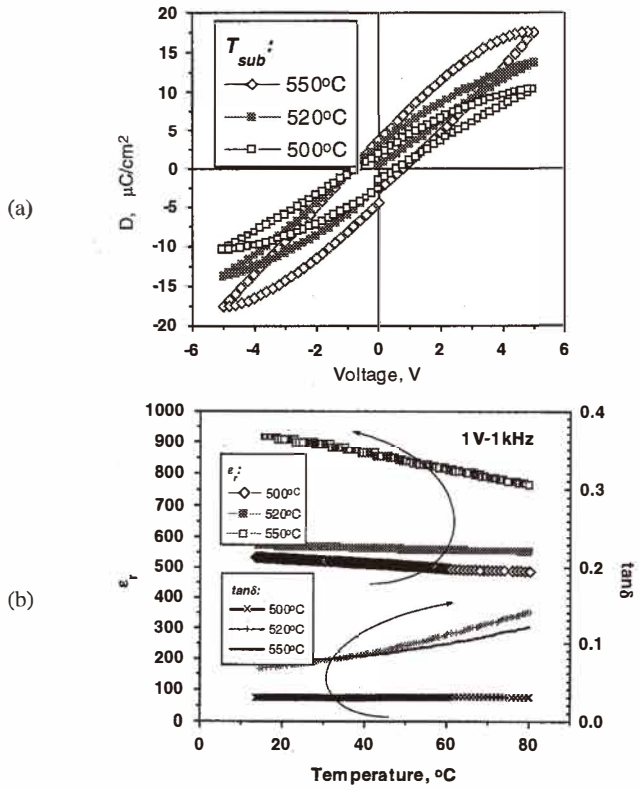

Fig. 6. T_{sub} dependence of ferroelectric properties of BST thin films prepared under optimized conditions. (a) Ferroelectric hysteresis loops and (b) relative dielectric constant and tangent loss.

The influence of dielectric loss on the measured TCD is quite delicate. The tendency is that lossy capacitors favor higher TCDs. Nevertheless, the deposition conditions for lossy or slightly leaky BST films cannot provide good reproducibility. It is considered that the high TCD partly results from an additional effect of the dependence of dielectric leakage on temperature. Thin film is a special case for application in dielectric bolometers because the dielectric leakage will be much more critical than that in bulk ceramics. Therefore, intensive attempts in the PLD-prototyping of 0.3-μm-thick bolometers were carried out recently to obtain BST films with higher TCDs. Typically, Fig. 8 shows the best properties achieved thus far in a 0.3-μm-thick BST film. The uniformity is about $\pm$6% within 6 elements in a Si(100)-chip. According to the D(T)-V and ε_r (tand δ)-T curves in Figs. 8(a) and (b), the bolometric effect in this sample is significant. When the temperature increases, the distinct decrease in the slope of the D-E loops agrees well with the monotonous decrease in dielectric constant. A high TCD value of about -1%/K is obtained, and the TCD has little dependence on the applied voltage (field). The increased value of tand δ might be due to dielectric leakage when the sensing amplitude voltage

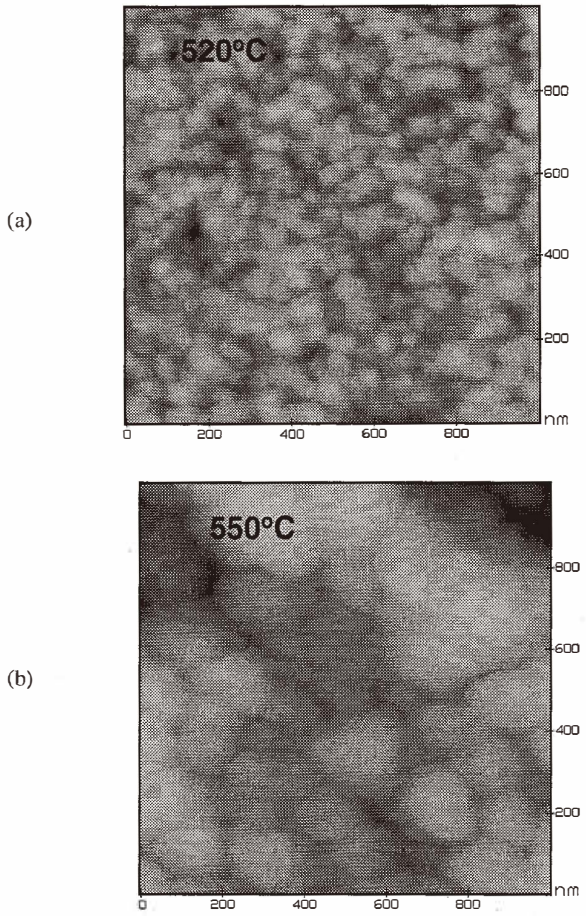

Fig. 7. AFM morphologies of BST films deposited at T_{sub} of (a) 520°C and (b) 550°C.

increased to 5V. The value of ε_r increases a little with an increase in the sensing voltage amplitude, and the small increase is due to the ferroelectric nonlinearity of BST films.

4. Sensor Characterization

Figure 9 gives a schematic view of the experimental setup in measuring IR responsivity of the bolometers pixel by pixel. To evaluate the response speed of a pixel, a mechanical chopper was applied between the IR filter and the IR source with chopping frequency controllable from 1 to 300 Hz, although the chopping is unnecessary in principle. A narrow band-pass amplifier was used for signal extraction. In this way, the signal voltage

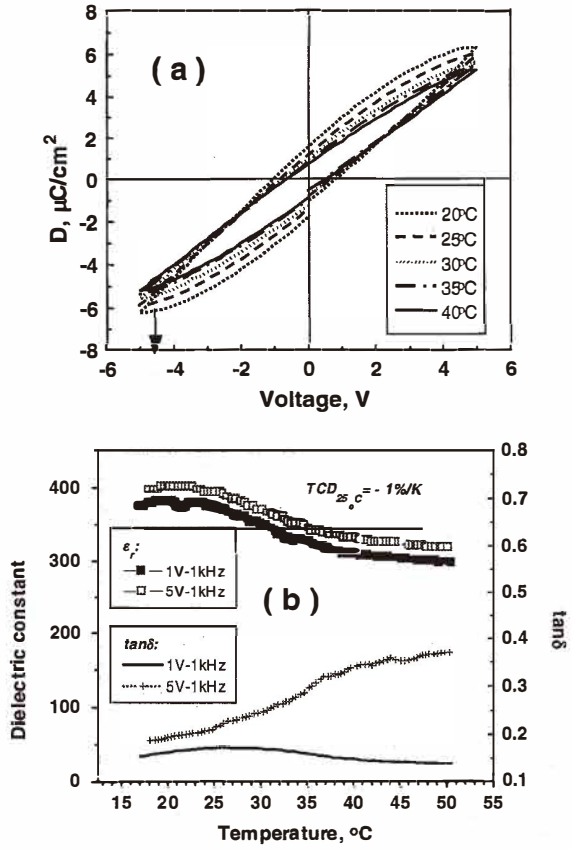

Fig. 8. The significant ferroelectric bolometric behavior shown by (a) ferroelectric hysteresis loops and (b) ε_r (tand δ)-T curves in a 0.3 μm BST thin film linear array fabricated on a micromachined test chip by PLD.

can be measured as a function of chopping frequency. For example, when a pixel with a TCD of 0.5%/K is exposed to an 80 mW/cm^2 infrared source, an output voltage change of 250 μV was detected at a chopping frequency of 5Hz. The waveform of the measured signals is shown in Fig. 10(a). Figure 10(b) shows the dependence of the signal voltage on the chopping frequency. The response is fast and the time constant τ_{th} was estimated to be about 8 msec, which is adequate for thermal imaging applications. The measured voltage sensitivity R_v was low at about 0.1 kV/W because we have not yet found a proper method to apply an IR-absorption layer (*e.g.*, Au-black) on the Pt/Ti upper electrode. As the noise voltage V_n was measured to be about 100 nV, a resultant specific detectivity of about 2×10^7 cm·VHz$^{1/2}$/W was obtained. These pixel performances are much lower than our estimations.[5] The unsatisfactory performance is thought to be due to the low IR

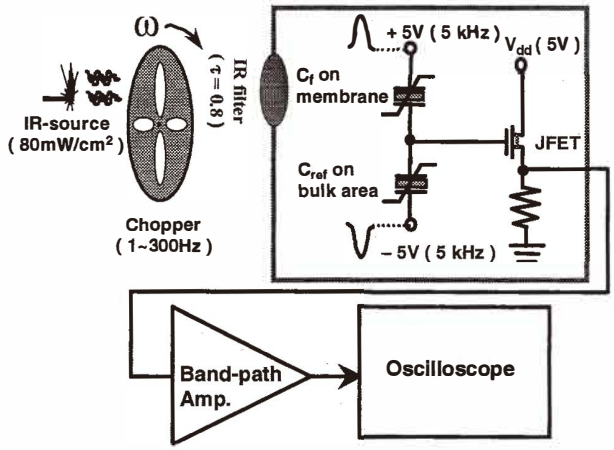

Fig. 9. The experimental arrangement used in the measurement of the detector output signal as a function of chopping frequency.

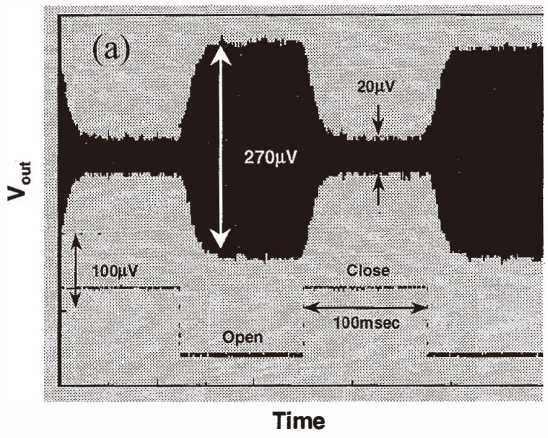

Fig. 10. (a) The as-detected signal waveform of one pixel upon the sensing area with and without IR-irradiation.

absorption efficiency of the bare Pt/Ti in our pixels. In fact, the absorption efficiency of our Pt/Ti was evaluated to be about 0.1. If Au-black could be applied, improvements 6 to 8 times as large as the above results in the signal voltage then in the detectivity can be expected.

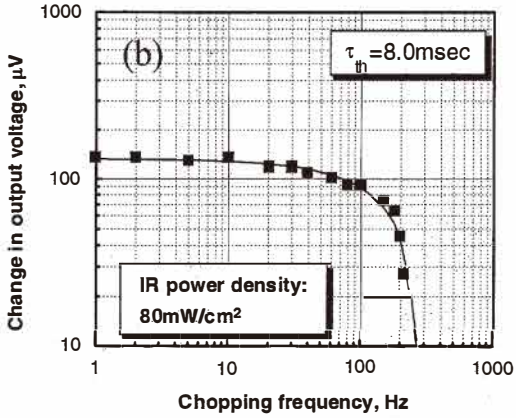

Fig. 10. (Continued) (b) The change of output voltage as a function of chopping frequency.

5. Conclusions

A monolithic process oriented to integrate IC fabrication, Si micromachining and deposition of BST sensor films has been developed. The ferroelectric microbolometer operating in a pulsed mode with a reference capacitor is capable of achieving better responsivity than in the DC-biased mode. Uncooled focal plane arrays based on this technology hold value-added advantages of chopperless operation and low power dissipation. A chopperless operation of pixels of a pulse-biased C-C bridge using BST ferroelectric microbolometers has been successfully confirmed. The resultant R_v and D^* were calculated to be about 0.8 kV/W and 1.6×10^8 cmHz$^{1/2}$/W, respectively, and the noise voltage (V_n) was 100 nV. The detectivities were not as satisfactory due to the low TCD value achieved in actual BST films because of the grain-size effect. Key issues for obtaining good performance as IR sensors are the improvement of bolometric performance of BST films by epitaxial growth or enlarging the grain size, development of new schemes for producing crack-free μm-thick BST films, and the implementation of surface IR absorbers. All these technical efforts will be directed towards improving the bolometric performance of BST film within the constraints of compatibility with monolithic Si-IC microfabrication and micromachining techniques.

Acknowledgements

One of the authors, H. Xu, would like to thank the Japan Science and Technology Agency for the STA fellowship support. We are grateful to Dr. K. Inoue, Mr. T. Nagashima, Mr. A. Tsutitani and Dr. S. Arita for their close collaboration and valuable discussions.

References

1 R. S. Balcerak: Proc. SPIE **3698** (1999)110–118.
2 W. Radford, D. Murphy, A. Finch, K. Hay, A. Kennedy, M. Ray, A. Sayed, J. Wyles, R. Wyles, J. Varesi, E. Moody and F. Cheung: Proc. SPIE **3698** (1999) 119–130.
3 P. W. Kruse and D. D. Skatrud: Uncooled Infrared Imaging Arrays and Systems, Semiconductors and Semimetals **47** (San Diego, Academic Press, 1997).
4 D. E. Witter, H. R. Beratan, B. M. Kulwicki and A. Amin: TI Technical Journal, Infrared Technology Sept-Oct. (1994) 19–26.
5 M. Noda, K. Hashimoto, R. Kubo, H. Tanaka, T. Mukaigawa, H. Xu and M. Okuyama: Sensors and Actuators A **77** (1999) 39–44.
6 H. Xu, T. Mukaigawa, K. Hashimoto, R. Kubo, T. Kiyomoto, H. Zhu, M. Noda and M. Okuyama: Proc. Transducers '99 **1** (1999) 398–401.
7 H. Xu, H. Zhu, K. Hashimoto, T. Kiyomoto, T. Mukaigawa, R. Kubo, Y. Yoshino, M. Noda, Y. Suzuki and M. Okuyama: Vacuum (in press) 2000.